Biophysical Chemistry 27 (1987) 131–138
Elsevier

BPC 01164

Conformations and selective photodissociation of heterogeneous benzo(*a*)pyrene diol epoxide enantiomer-DNA adducts

David Zinger [a,*], Nicholas E. Geacintov [a] and Ronald G. Harvey [b]

[a] *Chemistry Department, New York University, New York, NY 10003 and* [b] *The Ben May Laboratory for Cancer Research, The University of Chicago, Chicago, IL 60637, U.S.A.*

Received 3 November 1986
Accepted 3 March 1987

Benzo(*a*)pyrene diol epoxide; Stereoisomer; DNA adduct; Fluorescence; Linear dichroism; Conformation; Photodissociation

The covalent binding of the tumorigenic (+) enantiomer and the nontumorigenic (−) enantiomer of *trans*-7,8-dihydroxy-*anti*-9,10-epoxy-7,8,9,19-tetrahydrobenzo(*a*)pyrene (BPDE) to double-stranded native DNA gives rise to heterogeneous adducts, especially in the case of (−)-BPDE. The covalent (+)-BPDE-DNA adducts are predominantly of the external site II type, while the (−)-BPDE-DNA adducts are predominantly of the quasi-intercalative, site I type (65%), with 35% of site II adducts. The site I adducts can be selectively photodissociated with near-ultraviolet light (quantum yields in the range 0.0003–0.005); the external site II adducts (photodissociation quantum yield 3×10^{-5}) are 10–100-times more stable. The photolability of covalent (−)-BPDE-DNA adducts accounts for the discrepancies in the linear dichroism properties of these complexes reported previously. Fluorescence quenching data, previously utilized to assess the degree of solvent exposure of the pyrenyl residues in covalent adducts, were in some cases significantly influenced by the presence of highly fluorescent tetraol dissociation products. After correcting for this effect, it is shown that the fluorescence of the external site II (+)-BPDE-DNA adducts is sensitive to acrylamide, while the fluorescence of the dominant site I (−)-BPDE-DNA adducts is not affected by this fluorescence quencher, as expected for adducts with considerable carcinogen-base stacking interactions.

1. Introduction

The ultimate tumorigenic form of the well-known environmental pollutant benzo(*a*)pyrene, is the (+) enantiomer of the metabolite *trans*-7,8-dihydroxy-*anti*-9,10-epoxy-7,8,9,10-tetrahydrobenzo(*a*)pyrene (BPDE) [1–4]. There is a general view that mutagenesis and the initiation of tumorigenesis are related to the covalent binding of these and other polycyclic aromatic diol epoxides to cellular DNA [5]. The biological activities of these metabolites are not only a function of the total quantities of DNA adducts generated, but also depend on the specific nature of the different covalent reaction products which are formed with DNA [6–11]. Stereoisomeric diol epoxides, especially the (+) and (−) enantiomers of BPDE (fig. 1), provide a striking example of structure-biological activity relationships. In Chinese hamster V79 cells the mutagenicity of the (+) isomer is about 4-times greater than that of the (−) enantiomer for the same absolute level of covalent binding to DNA [7]; this difference was attributed by Brookes and Osborne to differences in the spatial orientation of the pyrenyl residue at the covalent binding sites, rather than to the observed differences in the chemical structures of the adducts formed.

Utilizing linear dichroism [12–14] and other spectroscopic approaches [15,16], striking differences in the conformations of adducts derived

Correspondence address: N.E. Geacintov, Chemistry Department, New York University, New York, NY 10003, U.S.A.
* Present address: Biology Department, Brookhaven National Laboratory, Upton, NY 11973, U.S.A.

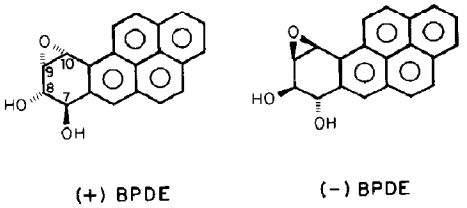

Fig. 1. Structures of the two enantiomers of BPDE.

from the covalent binding of the (+)- and (−)-BPDE enantiomers to DNA have indeed been observed. The conformations of BPDE-DNA adducts can be interpreted in terms of the site I/site II model [17]. Site I appears to involve intercalation, or partial intercalation of the pyrenyl chromophore between base-pairs, while site II corresponds to an external binding site, or to the localization of the pyrenyl moiety in a disordered region of the double helix [18]. The (+)-BPDE-DNA adducts are predominantly of the site II type, while the (−) adducts appear to be mixtures of site I/site II adducts [12–14]. The occurrence of site II adducts is correlated with high tumorigenicity and mutagenicity in mammalian cell systems, at least in the class of epoxides derived from the oxidative metabolism of benzo(*a*)pyrene [12–14, 17,18].

In this work, it is shown that near ultraviolet light (340–350 nm) of relatively low fluence rates (0.1 mW cm^{-2}) causes a selective photodissociation of site I adducts, while site II adducts are considerably less photolabile. The photoproducts, whose properties are consistent with those of the tetraols derived from the hydrolysis of BPDE, are highly fluorescent. This photodissociation effect can account for the previous discrepancies in the reported fluorescence properties of covalent BPDE-DNA adducts in aqueous solutions [19–22], as well as for the discrepancies in the absorption and linear dichroism properties of the adducts derived from the covalent binding of (−)-BPDE to DNA [12–14]. Fluorescence quenching techniques are utilized to show that pyrenyl residues characterized by site I conformations, which are dominant in (−)-BPDE-DNA adducts, appear to be less accessible to the solvent environment than site II adducts.

2. Materials and methods

The (+) and (−) enantiomers of BPDE were obtained from the National Cancer Institute Chemical Carcinogen Reference Standard Repository (lot nos. 83-344-49-5 (+), and 83-344-99 (−)), and dissolved in tetrahydrofuran (THF). The covalent BPDE-DNA adducts were prepared using native, double-stranded calf thymus DNA, as previously described [12,13]. All measurements were performed in solutions of 5 mM sodium cacodylate buffer (pH 7.0) at 24 ± 1°C.

The linear dichroism measurements were performed as described previously [13], utilizing a Couette cell to orient the DNA molecules in a flow gradient. The linear dichroism is defined as $\Delta A = A_{\parallel} - A_{\perp}$, where $A_{\parallel}$ and $A_{\perp}$ are the absorbances measured with the polarization vector of the incident light oriented parallel or perpendicular, respectively, to the flow direction. The ultraviolet irradiation and fluorescence measurements were performed utilizing a Spex 1902 Fluorolog fluorescence spectrophotometer (Spex Industries, Edison, NJ), interfaced with a microprocessor. The absolute light fluences incident on the samples in the spectrofluorometer were determined by means of an EG&G 100B photodiode which had been previously calibrated by means of a National Bureau of Standards tungsten filament lamp.

3. Results and discussion

3.1. Characteristic linear dichroism spectra

The linear dichroism spectra of site I and site II type adducts or complexes are shown in fig. 2A. Site I is best characterized by the linear dichroism spectrum of the noncovalent BPDE-DNA complexes formed immediately after adding BPDE to DNA solutions [13]; the in-plane transition moments of the pyrenyl chromophore tend to be tilted away from the DNA axis, and thus ΔA is negative for site I adducts. Site II adducts are best characterized by the covalent adduct derived from the covalent binding of (+)-BPDE to DNA [12]; the dichroism is positive, suggesting that the long

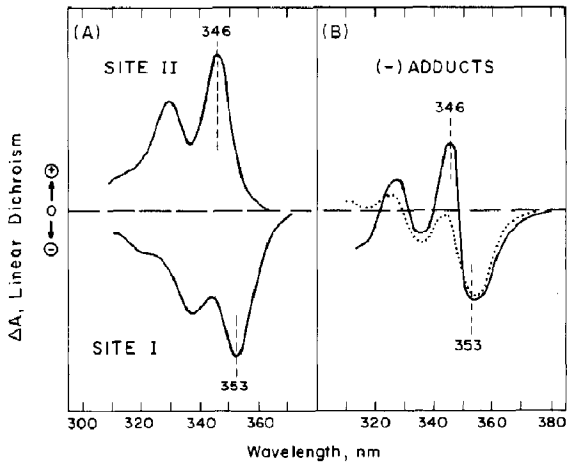

Fig. 2. (A) Characteristic linear dichroism spectra of site I (noncovalent, intercalative BPDE-DNA complexes, as in ref. 13, and site II (covalent adduct derived from the binding of (+)-BPDE to DNA [12]). (B) Examples of linear dichroism spectra of two different adducts derived from the binding of (−)-BPDE to DNA; (———) from ref. 12, (· · · · · ·) another sample of undefined history of exposure to ambient light (see also ref. 14 in which a similar spectrum of covalent (−)-BPDE-DNA adducts is shown).

axis of the pyrene-like chromophore is tilted closer towards the DNA axis.

In contrast to the covalent (+)-BPDE-DNA adducts, the published linear dichroism spectra of the (−)-BPDE-DNA adducts are variable in shape [12–14,18]. An example of such differences observed with two different adduct preparations is shown in fig. 2B. As described elsewhere [12], these ΔA spectra appear to be superpositions of site I and site II linear dichroism spectra. Positive extrema in the 325–330 nm range coincide with the positive ΔA peaks at 329–330 and 345–346 nm due to site II, while the minima occur at 336 and 354 nm, which coincide with the negative ΔA maxima due to site I. The history of the two samples whose ΔA spectra are depicted in fig. 2B, in particular their previous exposure to ambient illumination, was not monitored; it is shown below that these differences in the linear dichroism spectra are due to a selective photodissociation of site I chromophores which can give rise to varying proportions of site I and site II in a given sample of (−)-BPDE-DNA adducts. The higher the relative proportion of site II adducts, the more pronounced are the positive linear dichroism signals near 327 and 345 nm.

3.2. *Photodissociation of adducts detected by fluorescence*

In the course of investigating the fluorescence properties and the discrepancies in the ΔA spectra of different (−)-BPDE-DNA samples, it was found that the higher proportions of site II ad-

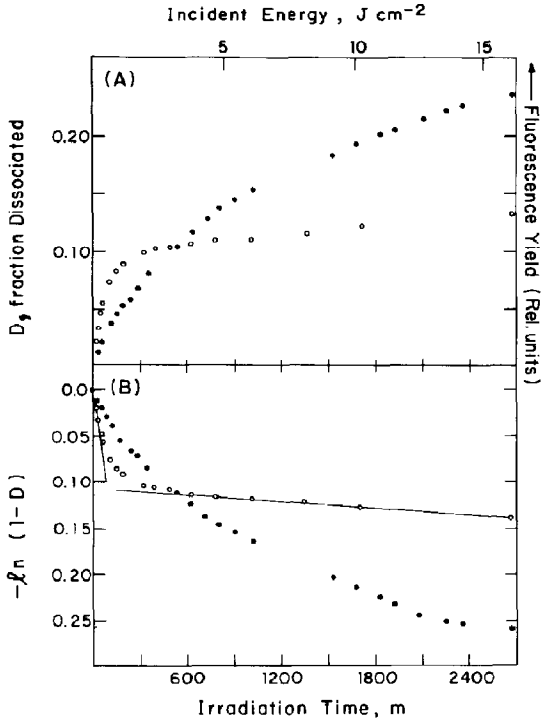

Fig. 3. (A) Time dependence of appearance of fluorescent dissociation products (tetraols) as a function of exposure to light (343±20 nm, 0.1 mW cm^{-2}, 1 cm path length, 1 ml irradiated volume. (○) (+)-BPDE-DNA covalent adducts, 9.9×10^{-4} M DNA concentration (in nucleotides) and 3.9×10^{-6} M covalently bound pyrenyl chromophores. (●) (−)-BPDE-DNA covalent adduct (7.5×10^{-4} M DNA and 1.3×10^{-6} M pyrenyl chromophores). Samples in 5 mM sodium cacodylate buffer (pH 7.0) at 25°C. (B) Data in panel A plotted according to eq. 1.

ducts, as determined from the linear dichroism and absorption spectra [12], are correlated with high apparent fluorescence yields. In fact the fluorescence yields of such solutions depend on the previous exposure of the samples to ultraviolet light; the fluorescence yields of freshly prepared adduct solutions increase as a function of illumination time in the spectrofluorometer (fig. 3A). In the case of the (−) adducts, the fluorescence yield increases gradually and continuously as a function of illumination time. This increase in fluorescence yields is due to ether-extractable products, since repeated extractions of the irradiated solutions caused a sharp decrease in the fluorescence yields. The ether extracts displayed both the absorption and fluorescence properties of the tetraol hydrolysis products 7,8,9,10-tetrahydroxytetrahydrobenzo(*a*)pyrene (BPT); furthermore, the relatively highly fluorescent, ether-extractable dissociation products exhibit the same high-performance liquid chromatography elution profiles as BPT on a Whatman Partisil ODS-3 column using a 3:7 water/methanol solvent mixture and a constant flow rate of 1 ml/min. Therefore, the dissociation products are most likely to be tetraols. In their studies of acid-induced dissociation of adducts, Dipple et al. [23] found that 7,12-dimethylbenz(*a*)anthracene-modified DNA adducts are acid-labile, and that the dissociation products are the 1,2,3,4-tetrahydrotetrahydroxy derivates of 7,12-dimethylbenz(*a*)anthracene [23].

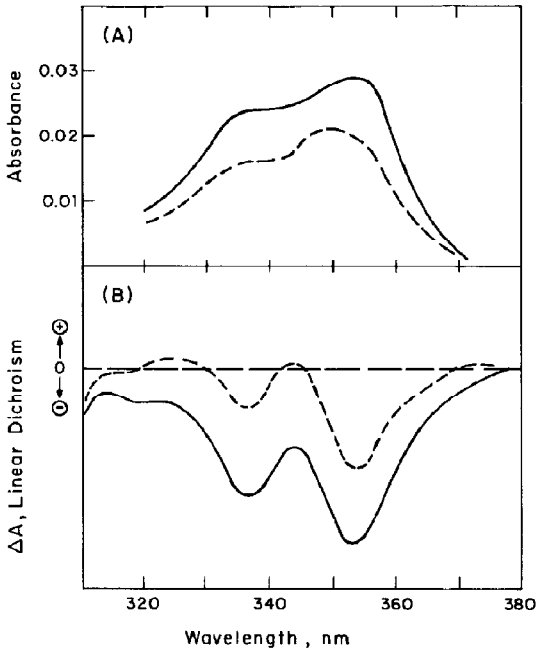

Fig. 4. Absorption (A) and linear dichroism spectra (B) of a covalent adduct derived from the binding of (−)-BPDE to DNA before (———) and after (------) irradiation (total irradiation dose of 26 J cm^{-2}). Same (−)-BPDE-DNA covalent adduct sample as in fig. 3.

3.3. Kinetics of photodissociation and nature of adducts

The per cent dissociation of the adducts was deduced from a determination of the decrease in absorbance of the adducts as a function of irradiation time (a typical result is shown in fig. 4A), and the amount of dissociation products determined from a quantitative analysis of the increased fluoresence yield (utilizing tetraol solutions of known concentration as standards). There may be some photobleaching of the pyrenyl chromophores, since only about 80–90% of the dissociation products are recovered as tetraols. In the laser photobleaching experiments of Boles and Hogan [24], on the other hand, a complete bleaching of the pyrenyl chromophores was observed under presumably higher fluence rates.

In the case of a single component-DNA adduct, undergoing dissociation according to first-order kinetics, the following linear relationship is predicted:

$$-\ln(1-D) = k(I)t \qquad (1)$$

where D is the fraction of adducts dissociated, t the time, and $k(I)$ a rate constant which depends on the fluence rate I. Kinetic plots of the data according to this equation (fig. 3B) clearly show that there is a heterogeneity of dissociating adducts since the semilogarithmic plots are nonlinear. The (+) adducts are characterized by a fast component (1.2×10^{-3} min^{-1}) and a slow component (1.3×10^{-5} min^{-1}) when $I = 0.1$ mW cm^{-2}. Under the same conditions of illumination,

the (−) adducts are characterized by a greater heterogeneity of rate constants within the range of approx. $(4–40) \times 10^{-5}$ min^{-1}. It is well known that the composition of the (−) adducts is chemically more heterogeneous than that of the (+) adducts [7,25]; the (+) enantiomer binds mostly to N2 of deoxyguanine (94% of adducts), while the (−) enantiomer gives rise to 59% of N2-dG, 21% of 06-dG, and 18% of N6-deoxyadenine adducts [7]. Since only a small fraction of the (+) adducts appear to be highly susceptible to photodissociation, the N2-dG adduct is assumed to be the more stable one, characterized by a lower value of the rate constant $k(I)$. The quantum yield of photodissociation of the (+) adducts is estimated to be 3×10^{-3} (molecules of tetraols formed/photons absorbed) for the minor, photolabile adducts, and 3×10^{-5} for the more stable major N2-dG adduct. In the case of the more heterogeneous (−) adducts, the quantum yields lie in the range of $(3–50) \times 10^{-4}$.

Under conditions of exposure of the (−) adducts to ambient laboratory fluorescent lights at room temperature, the adduct photodissociation rate was found to be in the range 1–3%/h. In the absence of light, at room temperature, the dissociation rate is only 0.08 ± 0.02%/h in the case of both the (+) and (−) adducts. No significant dissociation, as detected by the sensitive fluorescence technique described here, was noted in the refrigerator (4°C, in the dark) for at least up to 2 months.

3.4. Changes in site I/site II composition of adducts due to ultraviolet irradiation

The absorption and linear dichroism characteristics of a freshly prepared (−) adduct, and the same adduct exposed to a total dose of 26 J cm^{-2} and extracted with ether, are shown in fig. 4 (about 33% dissociation occurred according to the decrease in the absorbance at 353 nm, and 28% according to the quantity of BPT formed). Before irradiation, the absorption maximum is located at 353 nm, whereas previously [12,14] only a shoulder was observed at this wavelength. The linear dichroism spectrum of the freshly prepared sample is also remarkably different from those previously published (refs. 12–14 and 18, and fig. 2B), and more closely resembles that of the intercalated, noncovalently bound site I complex (fig. 2A). After irradiation, the loss of chromophores is accompanied by a decrease in the negative ΔA signal, and the overall linear dichroism signal is slightly positive in the 320–330 and 345 nm regions, where positive peaks in ΔA due to site I occur (fig. 2A).

The observed changes in the absorption and linear dichroism characteristics can be explained in terms of a selective photodissociation of site I adducts, and a higher stability of the site II adducts. There is a greater decrease in the absorbance at 353 nm (33%) than at 346 nm (21%), and there are similar changes in ΔA. The positive contribution to the linear dichroism at 346 nm is more apparent after irradiation than before, and there is also a decrease in the dichroism at 353 nm. These changes indicate that there is a greater proportion of site II adducts after irradiation than in the freshly prepared sample. These results therefore account for the variability in the shapes of the linear dichroism spectra of (−) adducts reported previously [12–14,18] since, in the previous experiments, the illumination history of the samples was not controlled. Utilizing spectroscopic methods outlined earlier [12], the overall absorption spectrum of the (−) adducts can be decomposed into contributions due to sites I and II; a crude estimate at 65–70% of site I adducts can thus be obtained in the unirradiated samples, which is higher than the previous estimate of 45 ± 5% obtained with partially photodissociated (−) adduct samples [12].

3.5. Effects of tetraol dissociation products on fluorescence excitation profiles

Solutions of covalent BPDE-DNA adducts contaminated with tetraol dissociation products can be easily recognized by measuring the fluorescence excitation spectra. In these measurements the emission wavelength in the fluorometer is held constant at 380–420 nm, while the excitation wavelength is varied; in tetraol-contaminated solutions the maxima in the excitation spectra occur at 343 nm. Most of the tetraols can be extracted with ether, whereupon the maxima in

the fluorescence excitation spectra shift to longer wavelengths, and correspond more closely to the absorption maxima of the covalent adducts [26]. For example, Chen [27] reported that the fluorescence excitation maxima of covalent adducts derived from the binding of (+)-BPDE and of (−)-BPDE to native DNA occur at 344–346 nm. However, it is not clear to what extent, if any, the fluorescence excitation spectra measured by Chen were influenced by the presence of tetraol dissociation products.

The tetraols are characterized by an unusually long fluorescence lifetime (200 ns in oxygen-free solutions [19]). As a consequence, the fluorescence of tetraols is extremely sensitive to quenching by extraneous molecules such as oxygen [19,21] and acrylamide [18,22]. Most recent measurements of the fluorescence decay times of (+)- and (−)-BPDE-DNA covalent adducts utilizing synchrotron radiation light pulses show that the lifetimes of the covalently bound pyrenyl residues are characterized by fluorescence decay times of about 1.5 and 6–9 ns (D. Zinger, unpublished observations). These values of lifetimes are within the range of those reported for racemic BPDE-DNA adducts [21,28]. Since the fluorescence lifetimes of the covalently bound chromophores are shorter by factors of 22–130 than the decay time of the tetraol dissociation products, the fluorescence of the latter is much more strongly quenched than the fluorescence of the adducts, at a given quencher concentration.

Fluorescence excitation spectra of covalent (+)-BPDE-DNA and (−)-BPDE-DNA adducts are shown in fig. 5 (continuous lines). The maximum in the fluorescence excitation spectrum of the (+) adducts occurs at 346 nm (fig. 5A), in good agreement with the results of Chen [27]; in the presence of 0.6 M acrylamide, the fluorescence yield is reduced by a factor of 0.6 and the excitation maximum is shifted slightly to the red, to 347 nm (broken line in fig. 5A).

In the case of the (−)-BPDE-DNA adducts, the fluorescence excitation maximum occurs at 343 nm (fig. 5B, continuous line); a shoulder at 354 nm coincides with the absorption maximum (fig. 4A). Upon the addition of acrylamide (0.6 M), the overall fluorescence yield is reduced, the

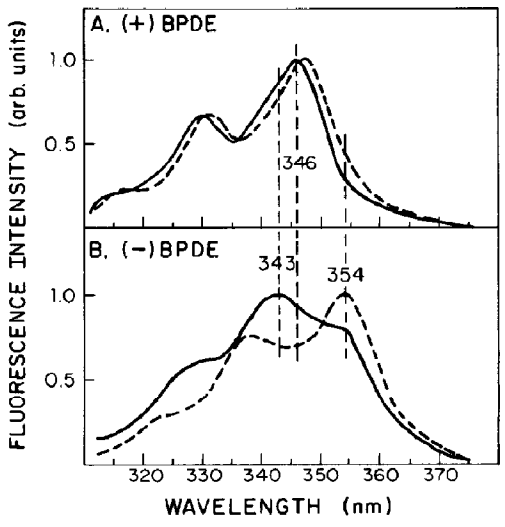

Fig. 5. Fluorescence excitation spectra of (+)-BPDE-DNA covalent adducts (8.0×10^{-6} M pyrenyl residues and 8.2×10^{-4} M DNA) and (−)-BPDE-DNA adducts (3.0×10^{-6} M pyrenyl residues and 7.5×10^{-4} M DNA). Excitation bandwidth, 4 nm; fluorescence viewing wavelength, 398 ± 5 nm. (———) No acrylamide; (- - - - -) 0.6 M acrylamide. The two spectra are normalized at the maxima; in panel A, the dashed spectrum was multiplied by a factor of 1.7, and in panel B by a factor of 1.4.

maximum in the excitation spectrum is shifted to 354 nm, and this spectrum (broken line, fig. 5) now more closely resembles the absorption spectrum, and the inverted linear dichroism spectrum (fig. 4) of the (−)-BPDE-DNA adducts. While Chen did observe a shoulder at 355 nm in the fluorescence excitation spectrum of (−)-BPDE-DNA adducts, the maximum at 344–345 nm was higher in intensity by a factor of about three [27]; this suggests that Chen's solutions were partially contaminated with tetraols. It is shown elsewhere [28] that the fluorescence properties of solutions of covalent BPDE-DNA adducts are severely distorted even when only small quantities of tetraols are present (1–2% of the total chromophores).

3.6. Differences in conformational properties studied by fluorescence quenching techniques.

The site I/site II model implies that the pyrene residues of BPDE bound covalently to double-

stranded DNA at these two types of binding sites should be characterized by different degrees of solvent exposure. The site I adducts, because of stacking interactions between the pyrenyl chromophores and the DNA bases, are predicted to be less accessible to solvent molecules, as well as to fluorescence quenchers dissolved in the solvent environment. Site II adducts, on the other hand, are predicted to be accessible [19]. These predictions can be verified by utilizing acrylamide as a fluorescence quencher [22]. The well-known Stern-Volmer equation [29]:

$$F(0)/F = 1 + \tau K[\mathrm{Acr}] \qquad (2)$$

predicts that the ratio of fluorescence yields in the absence ($F(0)$) and presence (F) of quencher should depend linearly on the acrylamide concentration ([Acr]), as long as there is only one chromophore. The slope of this plot is proportional to the fluorescence lifetime and the bimolecular encounter rate constant K. For free BPT in aqueous solution, the value of K is $7.5 \times 10^8\ \mathrm{M^{-1}\ s^{-1}}$ [26].

Stern-Volmer plots for (+)-BPDE-DNA and (−)-BPDE-DNA adducts are shown in fig. 6. An excitation wavelength of 352 ± 2 nm was selected for these measurements because it is (approximately) intermediate in value with respect to the absorption maxima of the (+)- and (−)-BPDE-DNA adducts. The plot for the (+) adducts exhibits downward curvature, and the Stern-Volmer quenching ratio increases gradually to a value of almost 1.5 as the acrylamide concentration is increased to 0.7 M. In contrast, in the case of the (−)-BPDE-DNA adducts, the $F(0)/F$ ratio rises to a value of about 1.2 as the acrylamide concentration is increased from zero to about 0.1 M. Further additions of acrylamide have no influence on the fluorescence yield of the (−)-BPDE-DNA adducts.

The initial rise in the $F(0)/F$ ratio observed in the case of the (−) adducts can be attributed to the quenching of the fluorescence of the tetraol contaminant. This conclusion is supported by the change in the fluorescence excitation spectrum as shown in fig. 5B. The constancy of the $F(0)/F$ factor as the acrylamide concentration is increased further indicates that the pyrenyl residues in the covalent (−)-BPDE-DNA adducts are not accessible to acrylamide, and are therefore not solvent exposed.

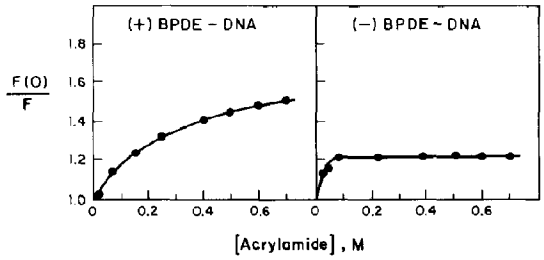

Fig. 6. Stern-Volmer fluorescence quenching ratios (see eq. 2) as a function of acrylamide concentration. Excitation wavelength, 352 ± 2 nm; fluorescence viewing wavelength, 398 ± 5 nm. Covalent (+)-BPDE-DNA adducts: 1.0×10^{-6} M pyrenyl residues and 1.0×10^{-4} M DNA. Covalent (−)-BPDE-DNA adducts: 3.0×10^{-7} M pyrenyl residues and 7.5×10^{-5} M DNA.

The pyrenyl chromophores in the (+)-BPDE-DNA adducts appear to be at least partially accessible to acrylamide, since $F(0)/F$ increases continuously as the acrylamide concentration is increased. The curvature of the plot is characteristic of samples of heterogeneous chromophores, in which case eq. 2 is no longer valid. Since the covalent BPDE-DNA adducts are characterized by two fluorescence decay times, downward-curving Stern-Volmer plots are expected. Detailed, quantitative analyses of Stern-Volmer plots are provided elsewhere [28].

The acrylamide fluorescence quenching profiles shown in fig. 6 are consistent with the dominance of site I conformations in adducts derived from the covalent binding of (−)-BPDE to DNA, and of site II external, or solvent-accessible conformations in DNA adducts derived from the binding of (+)-BPDE. Analogous conclusions have been reached from studies of the optical detection of magnetic resonance (ODMR) properties of covalent (+)-BPDE-DNA and (−)-BPDE-DNA adducts [30].

4. Conclusions

The absorption, linear dichroism, and fluorescence properties of covalent adducts derived from

the covalent binding of the (−) enantiomer of BPDE to DNA suggest a significant extent of overlap between the pyrene residues and the DNA bases. The wedge-shaped intercalation model at kinked DNA-binding sites, as suggested by Hogan et al. [22], could thus be applicable to the site I type of binding sites. However, in the case of adducts derived from the binding of the tumorigenic (+) enantiomer, site II binding, with very different spectroscopic characteristics, is dominant. The pyrenyl residues in site II conformations do not appear to be stacked with the DNA bases, and seem to reside at solvent-exposed DNA-binding sites; the properties of these adducts are therefore not consistent with those expected for wedge-shaped intercalation complexes.

The selective photodissociation effects described in this work can be utilized to correlate the conformational properties of heterogeneous BPDE-DNA adducts with their chemical composition. For example, it has been proposed that the site II species observed in the linear dichroism spectra of adducts derived from the binding of (−)-BPDE to DNA, which contributes a positive dichroism signal at 330 and 346 nm (fig. 4), are due to N2-dG species [12]. This hypothesis can be tested by photobleaching the site I adducts, and then subjecting the residual DNA adducts to chemical analysis. Such experiments are presently underway in our laboratory.

Acknowledgements

This research was supported by the U.S. Public Health Service, grant no. CA20851, awarded by The National Cancer Institute, DHHS, and by The Department of Energy (grant DE-FG02-86ER60405 and contract DE-AC02-78EV04959) at N.Y.U., and by The American Cancer Society (grant BC-132) and The National Cancer Institute (grant no. CA 36097) at The University of Chicago.

References

1 R.G. Harvey, Acc. Chem. Res. 14 (1981) 218.
2 A. Dipple, R.C. Moschel and C.A.H. Bigger, in: Chemical carcinogens, 2nd edn., ACS Monograph 182 (American Chemical Society, Washington, DC, 1984) p. 41.
3 A.H. Conney, Cancer Res. 42 (1982) 4875.
4 B. Singer and D. Grunberger, Molecular biology of mutagens and carcinogens (Plenum Press, New York, 1983).
5 I.B. Weinstein, A.M. Jeffrey, K.W. Jennette, S.H. Blobstein, R.G. Harvey, C. Harris, H. Autrup, H. Kasai, and K. Nakanishi, Science 193 (1976) 592.
6 J.C. Pelling, T.J. Slaga and J. DiGiovanni, Cancer Res. 44 (1984) 1081.
7 P. Brookes and M.R. Osborne, Carcinogenesis, 3 (1982) 1223.
8 R.F. Newbold, P. Brookes and R.G. Harvey, Int. J. Cancer 24 (1979) 203.
9 C.W. Stevens, N. Bouck, J.A. Burgess and W.E. Fahl, Mutat. Res. 152 (1985) 5.
10 W.E. Fahl, D.G. Scarpelli and K. Gill, Cancer Res. 41 (1981) 3400.
11 J.A. Burgess, C.W. Stevens and W.E. Fahl, Cancer Res. 45 (1985) 4257.
12 N.E. Geacintov, V. Ibanez, A.G. Gagliano, S.A. Jacobs and R.G. Harvey, J. Biomol. Struct. Dyn. 1 (1984) 1473.
13 N.E. Geacintov, H. Yoshida, V. Ibanez, S.A. Jacobs and R.G. Harvey, Biochem. Biophys. Res. Commun. 122 (1984) 33.
14 B. Jernström, P.O. Lycksell, A. Gräslund and Nordén, Carcinogenesis 5 (1984) 1129.
15 F.M. Chen, Biochemistry 24 (1985) 5045.
16 F.M. Chen, Biochemistry 24 (1985) 6219.
17 N.E. Geacintov, A.G. Gagliano, V. Ibanez and R.G. Harvey, Carcinogenesis 3 (1982) 247.
18 N.E. Geacintov, in: Polycylic hydrocarbons and carcinogenesis, ed. R.G. Harvey, ACS Symposium Ser. no. 283 (American Chemical Society, Washington, DC, 1985) p. 107.
19 T. Prusik, N.E. Geacintov, C. Tobiasz, V. Ivanovic and I.B. Weinstein, Photochem. Photobiol. 29 (1979) 223.
20 T. Prusik and N.E. Geacintov, Biochem. Biophys. Res. Commun. 88 (1979) 782.
21 O. Undeman, P.O. Lycksell, A. Gräslund, T. Astlind, A. Ehrenberg, B. Jernström, F. Tjerneld and B. Nordén, Cancer Res. 43 (1983) 1851.
22 M. Hogan, N. Dattagupta and J.P. Whitlock, Jr, J. Biol. Chem. 256 (1981) 4504.
23 A. Dipple, R.C. Moschel, M.A. Pigott and Y. Tondeur, Biochemistry 24 (1985) 2291.
24 T.C. Boles and M.E. Hogan, Proc. Natl. Acad. Sci. U.S.A. 81 (1984) 5623.
25 M.R. Osborne, S. Jacobs, R.G. Harvey and P. Brookes, Carcinogenesis 2 (1981) 553.
26 D. Zinger, Ph.D. Dissertation, New York University (1986).
27 F.M. Chen, J. Biomol. Struct. Dyn. 4 (1986) 401.
28 N.E. Geacintov, D. Zinger, V. Ibanez, R. Santella, D. Grunberger and R.G. Harvey, Carcinogenesis (1987) in the press.
29 J.R. Lakowicz, Principles of fluorescence spectroscopy (Plenum Press, New York, 1983).
30 V. Kolubayev, H.C. Brenner and N.E. Geacintov, Biochemistry 26 (1987) 2638.